



Universiteit
Leiden

The Netherlands

The electrochemical reduction of dioxygen and hydrogen peroxide by molecular copper catalysts

Langerman, M.

Citation

Langerman, M. (2021, October 12). *The electrochemical reduction of dioxygen and hydrogen peroxide by molecular copper catalysts*. Retrieved from <https://hdl.handle.net/1887/3217072>

Version: Publisher's Version

License: [Licence agreement concerning inclusion of doctoral thesis in the Institutional Repository of the University of Leiden](#)

Downloaded from: <https://hdl.handle.net/1887/3217072>

Note: To cite this publication please use the final published version (if applicable).

Chapter 1

Introduction to the role of molecular copper complexes as catalysts for the oxygen reduction reaction

1.1. Renewable energy and electrochemistry

Despite indications that the year-on-year growth of global greenhouse gas emissions has slowed down over the last 5 years, the atmospheric CO₂ levels keeps rising steadily.^[1] As a result global temperatures are expected to rise by as much as 2 °C by the second half of the 21st century, with lasting effects on the global climate.^[2-3] This will have dire consequences for a large part of humanity, especially for those living in low lying coastal areas due to rising sea levels,^[4-5] and in (near-) equatorial regions as a result of reduced precipitation in conjunction with an increase of extreme weather events.^[6] Furthermore, despite efforts to reduce or limit power consumption at a regional level, a significant increase (50%) in global energy demand is expected by 2050.^[7-8] This is projected to be largely the result of improvements in living conditions in Asia and the accompanied increase in energy demand. This signifies the importance of shifting to renewable energy sources to replace current fossil fuel energy sources and meet future energy demands in a short timeframe, to prevent future energy demand being fulfilled by traditional fossil fuel energy sources.

Renewable energy sources such as wind and solar energy will play an important part in this energy transition. With the use of photovoltaic solar cells, the abundant solar energy reaching Earth can be directly converted into electricity. The ease of scalability and the great affordability of this form of renewable energy makes it the prime candidate for sustainable energy generation. Increased generation of electrical energy will require significant electrification of transportation and industry via electrochemistry,^[9] as chemical feedstocks from fossil fuels will be significantly diminished. Additionally, the use of solar energy and, to a lesser degree, wind energy results in an increased intermittency of the power generation, influenced by the day-night cycle and seasonality of solar intensity.^[7, 10-11] This requires a way to quickly and efficiently store energy for use during periods of reduced electricity generation. Although battery technology has taken enormous strides in the last decade, especially in the automotive sector,^[12-13] large scale energy storage would ideally be done in the form of chemical energy. The storage of electricity in batteries is not easily scalable due to a linear increase in material cost with increasing capacity, while conversion to chemical energy can be done catalytically. Chemical energy can be stored in several different forms, such as methane, methanol, and dihydrogen; compounds that can be electrochemically converted to generate electricity, or vice versa. While not the most energy dense chemical, dihydrogen is one of the primary candidates as a renewable energy carrier, as only H₂, O₂ and H₂O are involved as chemicals, resulting in an environmentally friendly process without harmful waste. Additionally, hydrogen gas can readily be produced from water via the water splitting reaction, a process known since the 1839, when the first electrochemical cell was used to electrolyse water.^[14]

However, several technological challenges remain to be resolved in order to efficiently scale up and allow for the widespread adoption of electrolyzers and fuel cells.^[15-16] The most significant challenges are posed by the catalysts, electrode materials and certain energy inefficiencies in the involved electrochemical reactions.

1.2. The electrochemical oxygen reduction reaction

The oxygen reduction reaction (ORR) is one of the main efficiency-limiting catalytic reactions affecting the performance of fuel cells. The ORR is the driving-force behind the oxidation of fuels in different types of fuel cells, whether they are proton-exchange membrane fuel cells (PEMFC) or solid-oxide fuel cells (SOFC). In these fuel cells, dihydrogen (or another fuel, such as methane) is oxidized at the anode, resulting in the formation of protons and electrons, with the electrons generating an electrical current through an external circuit. These then reach the cathode, where they facilitate the reduction of dioxygen to water (Figure 1.1).

The theoretical maximum potential generated by such a hydrogen fuel cell is 1.23 V, as this is the standard reduction potential of O_2 (Scheme 1.1). However, limitations in the design of the fuel cell and the catalytic reactions themselves result in significant potential losses, thus limiting the efficiency of the fuel cell. While the hydrogen oxidation reaction (HOR) at the anode can be efficiently catalysed close the H^+/H_2 equilibrium by platinum catalysts with minimal overpotential losses, the ORR at the cathode is a significantly more complex multi-electron and multi-proton reaction involving several different reaction intermediates. Dispersed platinum nanoparticles on carbon (Pt/C) are currently used as ORR catalysts for application in fuel cells, but require high-catalyst loadings and suffer from poor long-term stability.^[17-18] Additionally, the

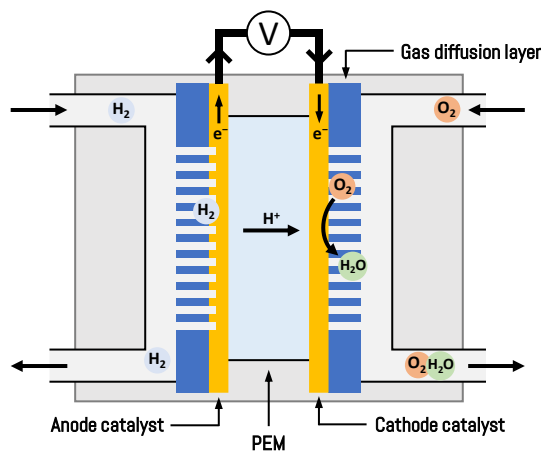


Figure 1.1. Simplified schematic representation of a PEM hydrogen fuel cell.

current state-of-the-art Pt ORR catalysts operate at overpotentials of more than 0.4 V.^[19-20] Thus, in contrast to the HOR, the ORR is one of the major contributing factors to the loss of efficiency due to sluggish reaction kinetics and the large overpotential required to reduce dioxygen to water.



Scheme 1.1. The two half-reactions responsible for generating electricity from hydrogen oxidation in a hydrogen fuel cell.

While there is significant interest in developing efficient Pt-free catalysts for the HOR to reduce the cost of fuel cells, the most significant gains in efficiency and price can be made through the development of better ORR catalysts, to both reduce the overpotential losses or find alternatives to the expensive Pt-based ORR catalysts. Several issues have to be overcome when developing new catalysts for the ORR. According to the Sabatier principle, the binding of the intermediate to the catalyst should be of intermediate strength, not too strong and not too weak, for optimal catalysis to occur.^[18, 21] However, for the ORR the binding strength of the metal catalyst to the intermediate OOH and OH species are very similar. Metals that destabilize the O-O bond of the metal-bound OOH intermediate by strengthening the M-OOH bond also show strong M-OH binding, which negatively impacts the reaction kinetics. This results in a specific optimum binding strength, where the optimal catalysts are guided by these scaling relationships. Nørskov *et al.* showed that Pt has the optimal binding strength with oxygen species, and thus has the best ORR activity and lowest overpotential of all transition metal catalysts.^[19] Many different alloys have been investigated as ORR catalysts since, but these still adhere to the scaling relations, hindering the development of more efficient heterogeneous metal catalysts.^[20, 22-23] To overcome the scaling relations associated with the ORR, catalysts would have to be developed that avoid the formation of the M-OOH intermediate. Alternatively, catalysts that are able to stabilize certain intermediates over others may lead to a more efficient catalytic reaction. This can be achieved by using three-dimensional catalysts, such as molecular catalysts, where a second coordination sphere around the metal centre can influence the stabilization of specific reaction intermediates.

1.3. Oxygen activation and reduction in natural systems

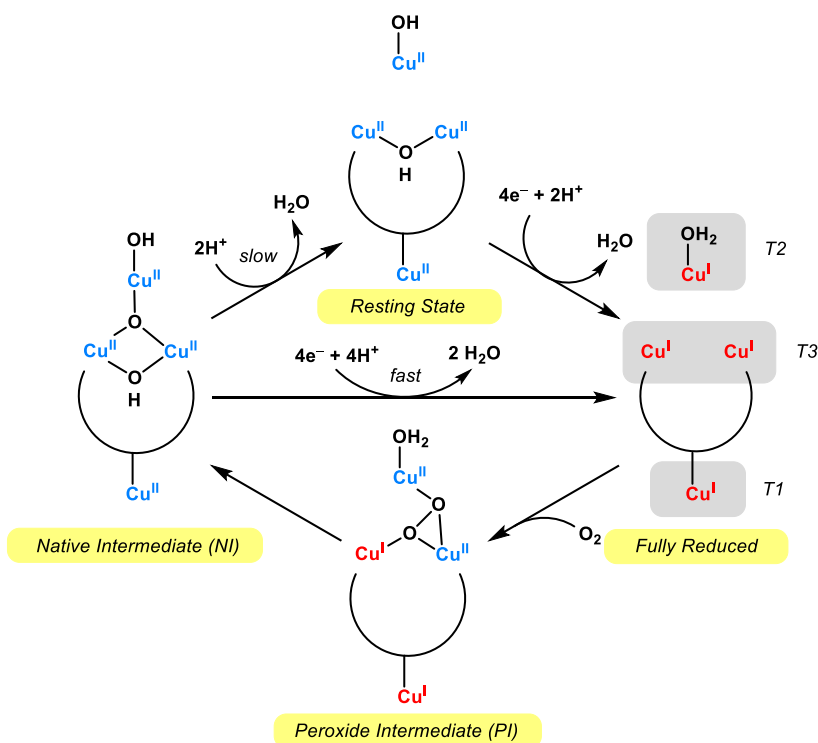
The active sites of enzymes are the perfect example of a three-dimensional catalyst. In these active sites substrates and reaction intermediates are stabilized or destabilized by interactions with amino acid moieties in the binding pocket, thereby tuning the

activation energies such that a catalytic reaction is optimized for a challenging cellular environment. Copper plays an important role in oxidoreductases, a family of redox-active metalloproteins responsible for catalysing reactions that involve electron transfer, where copper is the second most abundant metal after iron for these enzymes.^[17, 24-25] Examples of these copper-containing enzymes include lytic polysaccharide monoxygenases (LPMOs),^[26-31] particulate methane monoxygenase (pMMO),^[32-33] and multi-copper oxidases (MCO) such as tyrosinase, catechol oxidase and laccase.^[34-36] These enzymes activate and reduce dioxygen in order to oxidize a substrate, forming water in the process. The active sites of these copper-containing enzymes are classified in several types, based on their geometric and electronic structure.^[34] Type 1 (“blue copper”) centres contain a single copper ion in a trigonal-pyramidal or trigonal-bipyramidal geometry. Type 2 copper centres contain a single copper centre in a square-planar geometry. Finally, type 3 (dinuclear) copper centres contain two antiferromagnetically coupled trigonal-planar or trigonal-bipyramidal Cu centres bridged by a hydroxide ion in the resting state. Additionally, cytochrome c oxidase contains a mixed-metal dinuclear active site containing both a Cu (Cu_B) centre in a trigonal-pyramidal geometry and an Fe (heme α_3) centre. This enzyme catalyses the four-electron reduction of O_2 to H_2O in order to drive its proton pumping activity. In recent years a number of molecular models to mimic the cytochrome c oxidase catalytic centre have been created.^[37-38]

One MCO that has drawn significant interest in the context of the oxygen reduction reaction is Laccase, a multicopper enzyme capable of fully reducing O_2 to H_2O .^[34-35] In Laccase, the reduction of O_2 acts as the driving force for the oxidation of a wide range of phenolic substrates in plants, bacteria and fungi. The ORR in Laccase takes place at a trinuclear copper site, consisting of a type 2 (T2) copper centre and a type 3 (T3) copper centre, containing two copper ions. A third type (T1) copper site is present closer to the outside surface of the enzyme and is responsible for substrate oxidation. Electron transfer takes place over a distance of 14 Å between this T1 centre and trinuclear T2/3 cluster in the active site responsible for the ORR. The square-planar T2 copper centre contains two histidine ligands, while the tetrahedral T3 copper centres each have three histidine ligands and are bridged by a hydroxide group in the resting state, resulting in antiferromagnetic coupling between the two T3 copper ions. During the catalytic cycle for the reduction of O_2 by Laccase, the oxidized resting state, where all four copper ions are in a 2+ oxidation state, is first fully reduced via electrons supplied via the T1 copper site (Scheme 1.2).^[39-40] Upon reacting with dioxygen, a peroxide intermediate (PI) is formed, wherein peroxide is bridged between the three T2/T3 copper ions in the active site. After further electron-transfer steps, the O-O bond is cleaved, resulting in the native intermediate (NI) structure. Elimination of water from the NI state will regain the

resting state, or can preferentially lead straight to the fully reduced state if substrate oxidation is taking place, which allows for further electron transfer via the T1 site to the trinuclear centre.

Laccase has been used as a catalyst for the electrochemical ORR by immobilizing the enzyme on an electrode.^[41-47] These electrochemical studies revealed that Laccase is able to catalyse the reduction of dioxygen close to the ORR equilibrium potential, with a minimal overpotential of around 0.1 V. While this shows the thermodynamic efficiency of Laccase as an ORR catalyst, low current densities are achieved due to the large bulk of the enzyme leading to a low number of active sites per electrode surface area. While there have been successful attempts at increasing current density by incorporating Laccase into hydrogels or carbon aerogels, resulting in enzyme multilayers, slow electron transport limits the efficiency of such systems.^[42-43, 48] Whereas enzymes are important benchmarks for the electrocatalytic ORR, their practical application is limited due to the limited stability of the enzymes and the aforementioned low current densities, in comparison to heterogenous and molecular catalysts.

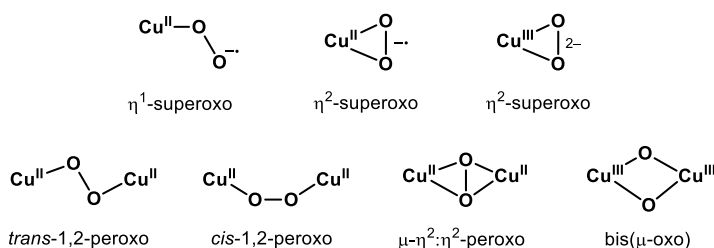


Scheme 1.2. Simplified schematic representation of the catalytic ORR mechanism of Laccase, showing only the main intermediates that have been detected via spectroscopic methods.^[39-40]

1.4. Molecular copper catalysts

Molecular complexes offer an opportunity to incorporate a ligand structure similar to those found in enzymes, while avoiding some of the efficiency-limiting downsides associated with the use of enzymes as electrocatalysts. Additionally, the reactivity of molecular complexes can be tuned by straightforward ligand modifications. The design of molecular catalysts is not only inspired by the active sites of enzymes, but molecular complexes often also serve as synthetic mimics for these active sites. Spectroscopic information of these model compounds is used to study the geometry, electronic structure, and the reactivity towards the binding of substrates to the metal centres to elucidate the reactions taking place in the active sites of enzymes.

The interaction of dioxygen and copper ions plays an important role in copper-containing enzymes that are able to reduce O_2 , and molecular compounds have been used to investigate these interactions. To study the formation of copper-dioxygen adducts, the reactivity of a wide range of Cu^I complexes with O_2 has been investigated.^[49-53] Several different binding modes of O_2 to copper centres have been identified (Scheme 1.3).^[54] The pyridylalkylamine copper complex $[Cu(tmpa)(L)]^+$ (Cu -tmpa; tmpa = tris(2-pyridylmethyl)amine), L = solvent molecule) is one of the earliest examples for which the formation of a copper-dioxygen adduct was proven using a combination of spectroscopic techniques.^[55-56] Using low temperature UV-vis absorption measurements and x-ray crystallography, Karlin *et al.* showed that the reaction between $[Cu^I(tmpa)(L)]^+$ and O_2 resulted in the formation of a dinuclear Cu_2-O_2 species. Follow-up studies using stopped-flow kinetic studies revealed that the formation of a short-lived copper(II)-superoxide complex precedes the formation of a *trans*- μ -1,2-peroxo complex.^[57-59] Exceedingly fast kinetics of the reaction between Cu^I and O_2 in aprotic solvents were measured.^[59] Following this report, a variety of different alkylamine and pyridylalkylamine complexes have been studied.^[50, 60-66] The generalized reaction pathway that was determined for reaction of these copper complexes with dioxygen follows the initial formation of a mononuclear $Cu^{II}-O_2^{\bullet-}$ adduct, followed by a dimerization step resulting in the formation of a bridged O_2^{2-} species.

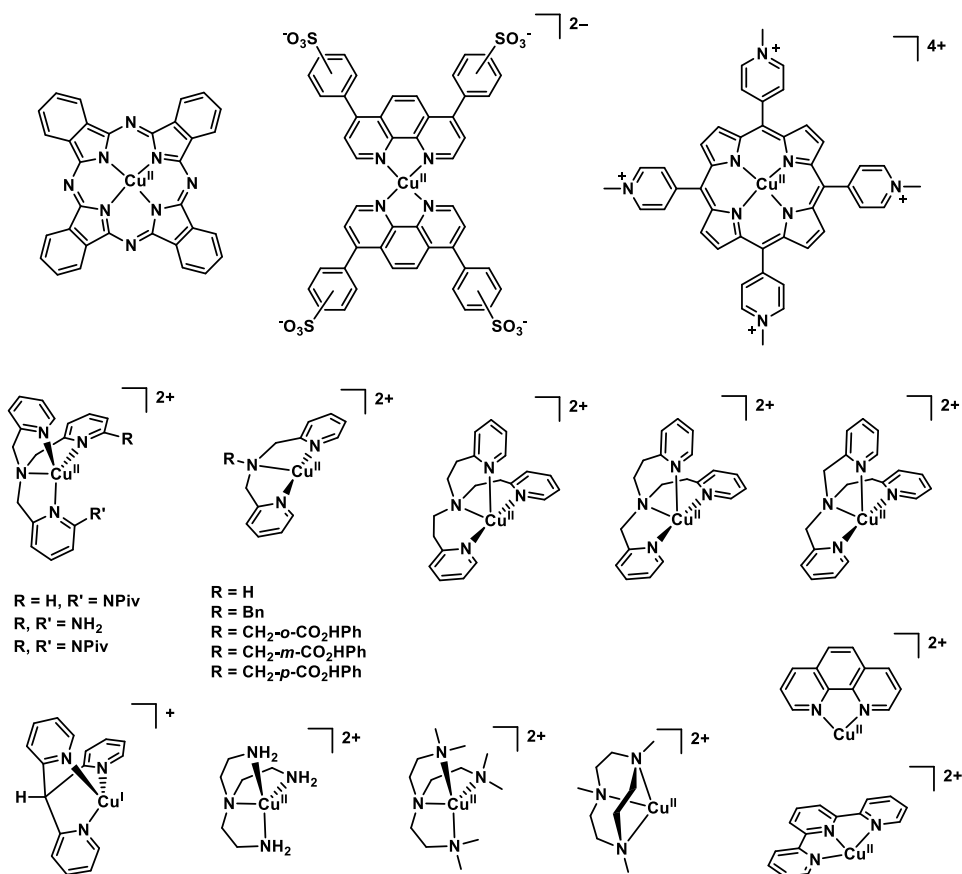


Scheme 1.3. Binding modes of dioxygen to copper.^[49]

Prior to the use of model copper complexes for the elucidation of reaction mechanisms of active sites in enzymes, copper complexes had already been studied as novel catalysts for the electrochemical reduction of O₂.^[67-69] This was driven by the discovery by Jasinski of a cobalt phthalocyanine complexes as a molecular catalyst for the ORR.^[70] Some of the earliest in-depth efforts to study the electrocatalytic reduction of O₂ by molecular copper complexes were performed by Anson *et al.*^[71-75] They showed that (substituted) phenanthroline copper complexes adsorbed on the surface of a graphitic electrode were able to catalyse the electrochemical ORR.^[71-72] Additionally, it was shown that a change in the coordination geometry took place upon reduction of the copper complex, from a square-pyramidal Cu^{II} to a tetrahedral Cu^I complex, even when absorbed on the electrode surface.^[71] Further research was performed on the electrocatalytic ORR by substituted phenanthroline copper complexes,^[76] including on phenanthroline copper complexes covalently bonded to the carbon electrode, which revealed a possible Cu₂O₂ intermediate during the ORR.^[77]

In the last decade the first biomimetic copper complexes have been investigated for their ORR activity, both using sacrificial chemical reductants and as electrocatalysts (Scheme 1.4).^[38, 78-93] Work by Karlin and Fukuzumi showed that Cu-tmpa is able to catalyse the ORR in acetone using ferrocene (Fc) as a reductant.^[78] It was observed that the peroxo dimer $[\{\text{Cu}^{\text{II}}(\text{tmpa})\}_2(\text{O}_2)]^{2+}$ is formed once all the perchloric acid is consumed by the catalytic reaction. Upon addition of more acid, this peroxo complex was also shown to be able to reduce dioxygen. Similar results were obtained for a substituted pyridylalkylamine complex $[\text{Cu}(\text{PV-tmpa})(\text{L})]^{2+}$, containing a pivalamido moiety on the ortho position of one of the pyridine arms.^[83] However, upon addition of the acid to the peroxo complex, its corresponding UV-Vis absorption band immediately disappeared. This was followed by a slower increase of the Fc⁺ absorption band, showing that catalytic reduction was taking place. This suggests that the monomeric Cu^{II}-OOH was formed upon addition of the acid, from which further reduction to H₂O proceeded. It was shown that the catalytic ORR rate constant of $[\text{Cu}(\text{PV-tmpa})(\text{L})]^{2+}$ was significantly larger than that of Cu-tmpa. However, differences in the ability of the acetate ion to coordinate to the copper centres between these two different complexes played an important role, and the use of non-coordinating acids could have a significant effect upon the relative rate constants. For the related $[\text{Cu}(\text{tepa})]^{2+}$ (tepa = tris[2-(2-pyridyl)ethyl]-amine) complex, it was shown that formation of a dinuclear copper peroxo intermediate is not a prerequisite to facilitate the 2-electron reduction of O₂ to H₂O₂, as this species was not observed.^[81]

The ORR by Cu-tmpa in aqueous buffered solutions was also investigated using electrochemical methods by Gewirth *et al.*^[84-85] Cu-tmpa and several other pyridylalkylamine complexes were incorporated into a carbon black (Vulcan XC-72) ink



Scheme 1.4. Schematic drawing of mononuclear copper complexes that have been reported to reduce dioxygen, either in the presence of chemical reductants or under electrochemical conditions.^[67-69, 71-93] Counterions and coordinating solvent molecules are omitted for clarity.

and dropcasted on a glassy carbon electrode. Comparison of the different pyridylalkylamine copper complexes showed minimal differences between catalysts in the onset of the ORR and the limiting currents above pH 4 during hydrodynamic voltammetry measurements using rotating ring-disk electrodes.^[85] At pH 4 and below, more significant differences were observed, with only Cu-tmpa maintaining its 4-electron ORR performance. However, based on experiments where Cu-tmpa was used as a homogenous ORR catalyst in solution, it was shown that Cu-tmpa is not stable in electrolyte solutions with a pH below 4, even under non-catalytic conditions.^[87] This raises questions concerning the nature of the catalysts that is present in heterogenized form under acidic conditions.

It was suggested that Cu-tmpa dimerizes upon reduction in the presence of dioxygen, based on an apparent shift in the onset potential of the ORR under rotating

conditions of the rotating ring disk electrode (RRDE),^[84] and the previously discussed studies on Cu-tmpa in organic solvents. However, the current at a given fixed potential always decreases proportional to the decrease in catalyst concentration under conditions where substrate is not limiting. This will result in a shift of the “apparent onset” of the catalytic reaction to lower potentials as a function of decreasing catalyst concentration, if a fixed current density is used as a reference to determine the onset potential. Furthermore, the catalytic onset potential is generally an ill-defined property.^[94] Indeed, the same data showed that the half-wave potential of the catalytic curve did not appear to shift as a function of catalyst loading, which is a more appropriate property to observe possible changes in electrocatalytic mechanisms.

A dinuclear copper complex containing two 3,5-diamino-1,2,4-triazole (dat) ligands (Cu-dat) has been considered a benchmark for molecular electrocatalytic ORR performance. In molecular form both copper centres are spaced similarly to the T3 copper centres present in Laccase.^[95] Gewirth *et al.* reported an ORR onset at 0.86 V vs. RHE at pH 13 which is the lowest reported overpotential for any copper catalyst.^[96] However, the species that was used in this study was formed by mixing a 2:1 ratio of ligand to Cu^{II} salt with carbon black, followed by dropcasting onto a glassy carbon electrode. This procedure did not correspond to the ratios used in the studies to investigate the structure of Cu-dat species.^[95] Our group has recently shown that the catalytic activity of the Cu-dat compound is largely the result of the formation of amorphous Cu⁰ and Cu^I depositions on the electrode surface, and can therefore not be ascribed to the molecular structure of the complex.^[97] These findings showcase some of the issues that arise when analysing molecular (electro)catalyst and the difficulty in transferring and applying results obtained under different experimental conditions to an electrocatalytic system.

1.5. Benchmarking the performance of homogeneous electrocatalysts using electrochemical methods

With the increased interest in molecular electrocatalysts for small molecule conversion (H₂, O₂, H₂O, CO₂) for renewable energy applications, it is necessary to have a robust framework to elucidate catalytic mechanisms and quantify the performance of molecular catalysts to allow comparisons between different catalysts. This has been an important topic in the field and has been highlighted in many publications in the last decade.^[98-107] Molecular electrocatalysts have been studied under a wide range of experimental conditions, utilizing different solvents, solution pH, and supporting electrode materials.^[108-110] The specific conditions in which molecular homogeneous electrocatalysts are evaluated using electrochemical techniques are often dictated by the solubility or stability of the catalyst under the chosen conditions. Thus, many

molecular electrocatalysts are evaluated in organic solvents, such as MeCN or DMF. Yet, in the context of renewable energy applications, water solubility is considered an important property in the development of new molecular catalysts, as is the catalyst performance under aqueous conditions.^[111-117] Evaluating the efficiency of a catalyst does not only require the determination of the kinetic performance in the form of catalytic rate constants or turnover frequencies, but also of the thermodynamic performance in the form of the catalytic onset potential or the overpotential relative to the equilibrium potential of the catalysed reaction. However, as mentioned in the previous section, the definition of the onset potential can be rather arbitrary or even not defined at all. These factors can hinder the benchmarking of electrocatalysts and makes comparisons between catalysts difficult.

Efforts have been made to standardize and rationalize the definition of the onset and overpotentials for molecular electrocatalysts.^[94, 118-120] The determination of the overpotential is relatively straightforward under ideal conditions, in which a voltammogram shows an S-shaped catalytic curve and the limiting plateau current is available. Here, the preferred measure of the catalytic potential for the determination of the overpotential is the catalytic half-wave potential ($E_{cat/2}$). This is the potential at which half the limiting or peak catalytic current is observed. In turn, the overpotential is defined as the difference between the equilibrium potential of the given reaction and the catalytic half-wave potential. Using the $E_{cat/2}$ as the measure for the catalytic potential results in smaller deviations when the catalytic systems behave less ideal.^[94] However, in the case of fast ORR electrocatalysts, mass transport limitations in O_2 can result in peak shaped catalytic currents that strongly deviate from an ideal S-shape, and where the mass transport independent plateau current is never reached. In these situations, the catalytic peak current can be reached before the redox potential of the catalytic species. Thus, an accurate description of $E_{cat/2}$ can only be obtained by using very high scan rates or by increasing the ratio of substrate to catalyst.^[107] In such cases the redox equilibrium potential ($E_{1/2}$) of the catalytic species or a well-defined onset potential at the start of the catalytic wave would be a better descriptor to determine the overpotential.

While the equilibrium potential of the catalysed reaction is well-established in aqueous solutions, this can be more challenging in non-aqueous solutions, where the H^+/H_2 reduction potential is not always known, or acid pK_a 's have not been determined. Several methods have been described to determine the overpotential in non-aqueous solutions.^[119-120] Recently, Roberts and Bullock reported a method to directly measure the equilibrium potentials of the H^+/H_2 couple in a given solvent without the need for the pK_a of the acid or the standard reduction potential $E_{H^+}^0$ in the particular solvent.^[121] This was followed by the determination of the standard reduction potential of O_2 in

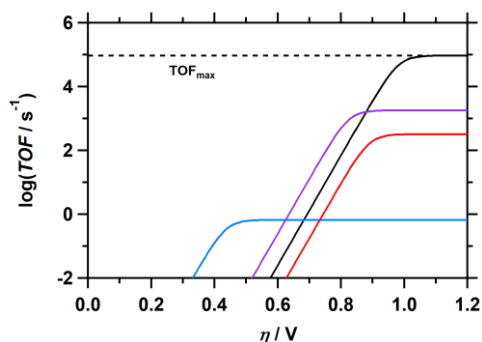


Figure 1.2. Simulated $\log\text{TOF}-\eta$ plot, showing the catalytic performance as a function of applied overpotential of several catalysts, each with a different TOF_{max} and catalytic overpotential.

acetonitrile and DMF using the same method by Mayer *et al.*^[122]

Another development is the introduction of the foot-of-the-wave analysis (FOWA) pioneered by Savéant and Costentin,^[123] which couples kinetic performance to the thermodynamic catalytic potential. As previously mentioned, side-phenomena such as substrate depletion and catalyst deactivation can result in significant deviation from the S shaped catalytic wave under purely kinetic conditions. This would result in underestimation of the observed rate constant. However, the FOWA can be used to analyse reactions where these side phenomena occur, as the catalytic current at the foot of the catalytic wave is considered to be purely kinetic in nature, without interference from side phenomena. Thus, the ideal or maximum rate constant can be derived from the foot of the catalytic wave. FOWA expressions for more complicated multi-electron multistep molecular electrocatalytic systems have also been proposed.^[98-100, 102, 124-125] It has to be noted that while FOWA is a very powerful tool, it is also very sensitive to the choice of the potential window used for the FOWA determination.^[124] The FOWA will be further discussed in Chapter 2. Maximum turnover frequencies (TOF_{max}) derived from the FOWA can be used to construct a $\log(\text{TOF})-\eta$ plot, where the $\log(\text{TOF})$ is plotted as a function of the applied overpotential (Figure 1.2). While the TOF_{max} of a catalyst is often never reached under experimental conditions, and will therefore be larger than the observed rate constants or TOFs, it can be useful in comparisons between catalysts. When multiple catalysts are compared in such a graph, overpotential zones can be identified in which particular catalysts show superior catalytic performance. It also highlights the trade-off between overpotential and the maximum catalytic rates of a catalyst. Therefore, these $\log(\text{TOF})-\eta$ plots, also called molecular Tafel Plots, can be a useful tool for comparing the catalytic performance of molecular electrocatalysts relative to the applied overpotential.^[105-106, 126-127]

1.6. Aim of research

The focus of the research described in this thesis is placed on the elucidation of electrocatalytic mechanisms of the ORR by homogeneous copper complexes. As discussed in the previous sections, a large knowledge base exists on the reaction of dioxygen with molecular Cu^I coordination complexes. Cu-tmpa is one of the most-studied catalysts for the chemical and electrochemical reduction of dioxygen, and is used as a reference for many other similar copper complexes. However, significant issues remain in translating mechanistic insights observed during chemical reduction to electrochemical systems, and vice versa, whereby heterogenized catalytic species have erroneously been ascribed a certain molecular character. An important question regarding Cu-tmpa is whether a dinuclear intermediate is required for the reduction of dioxygen under electrocatalytic conditions or whether this species is only present under non-catalytic conditions, something for which conflicting data was reported in previous electrochemical and non-electrochemical studies of the ORR. The limited understanding of the catalytic mechanism hinders the rational design of improved copper catalysts. Thus, we set out to elucidate the mechanism of the electrocatalytic ORR by Cu-tmpa under different conditions using a range of electrochemical techniques.

In Chapter 2, the mechanism of the electrochemical ORR by homogeneous Cu-tmpa in a neutral aqueous solution is discussed. The product distribution of the catalytic reaction as a function of the applied potential was determined using RRDE techniques. This revealed the formation of H₂O₂ as an intermediate product during the overall four electron reduction towards H₂O. Additionally, the catalytic performance was quantified, revealing one of the fastest reported rate constants for the ORR by a molecular catalyst. Finally, we show that a mononuclear species is responsible for the reduction of dioxygen, both in the FOWA potential window and at higher applied overpotentials. These results strengthen the notion that a dinuclear copper species is not required for fast oxygen reduction and illustrate the difficulties of transferring observations made under non-electrocatalytic conditions to an electrochemical system.

As it was shown that H₂O₂ plays an important role in the catalytic mechanism of the ORR, the research described in Chapter 3 builds upon the results of the previous chapter and elaborates on the reduction of hydrogen peroxide by Cu-tmpa in a neutral aqueous electrolyte solution. By comparing the catalytic performance between deuterated and non-deuterated solutions, a kinetic isotope effect (KIE) was determined. This revealed that the catalytic mechanism for the reduction of H₂O₂ follows a Fenton-like reaction pathway, wherein the formation of a copper(II) hydroxyl species and a free hydroxyl radical are involved in the rate-determining step. This shows

similarities with the mechanisms suggested for the active sites of several monocopper enzymes that show reactivity towards dioxygen and hydrogen peroxide.

The results described in Chapter 2 raised the question on whether the choice of solvent or proton source could be the main determinant for the catalytic mechanism, in relation to previous Cu-O₂ reactivity studies reported previously. In Chapter 4, it is shown that use of the strongly coordinating acetonitrile as an aprotic solvent slows down the electrocatalytic reduction of dioxygen by Cu-tmpa by several orders of magnitude. Using the previously discussed method to directly measure the equilibrium potential of the H⁺/H₂ couple, a slightly lower overpotential was observed compared to neutral aqueous solution. In contrast to previous suggestions, we show that even when the catalytic ORR is slowed down to a significant degree in acetonitrile, a mononuclear reaction mechanism is involved. This holds true in the presence of both coordinating and non-coordinating proton donors. Thus, we confirm that dimerization does not play a role in the electrocatalytic ORR by Cu-tmpa in water or acetonitrile under these conditions.

In Chapter 5, the electrocatalytic performance of several pyridylalkylamine copper complexes for the ORR and the reduction of hydrogen peroxide is discussed. The effect of changes in the ligand structure by varying ligand arm lengths on the redox chemistry and catalytic rates were investigated. Scaling relations were observed between the redox potentials of the catalysts and the maximum catalytic rate constants determined via FOWA, for both the reduction of dioxygen and hydrogen peroxide. This also coincides with a positive shift of the onset and $E_{cat/2}$ potentials corresponding with an increase in redox potential, thus resulting a significant reduction of the ORR overpotential compared to Cu-tmpa.

1.7. References

- [1] P. Friedlingstein, et al., *Earth Syst. Sci. Data* **2020**, *12*, 3269-3340.
- [2] IPCC, **2014**: *Climate Change 2014: Synthesis Report. Contribution of Working Groups I, II and III to the Fifth Assessment Report of the Intergovernmental Panel on Climate Change*, [Core Writing Team, Rajendra K. Pachauri, Leo Meyer (Eds.)]. IPCC, Geneva, Switzerland.
- [3] IPCC, **2018**: *Global Warming of 1.5°C. An IPCC Special Report on the impacts of global warming of 1.5°C above pre-industrial levels and related global greenhouse gas emission pathways, in the context of strengthening the global response to the threat of climate change, sustainable development, and efforts to eradicate poverty*, [V. Masson-Delmotte, P. Zhai, H.-O. Pörtner, D. Roberts, J. Skea, P.R. Shukla, A. Pirani, W. Moufouma-Okia, C. Péan, R. Pidcock, S. Connors, J.B.R. Matthews, Y. Chen, X. Zhou, M.I. Gomis, E. Lonnoy, T. Maycock, M. Tignor, T. Waterfield (Eds.)]. In Press.
- [4] M. I. Voudoukas, L. Mentaschi, E. Voukouvalas, M. Verlaan, L. Feyen, *Earth's Future* **2017**, *5*, 304-323.
- [5] R. S. Nerem, B. D. Beckley, J. T. Fasullo, B. D. Hamlington, D. Masters, G. T. Mitchum, *Proc. Natl. Acad. Sci.* **2018**, *115*, 2022-2025.
- [6] T. Weber, A. Haensler, D. Rechid, S. Pfeifer, B. Eggert, D. Jacob, *Earth's Future* **2018**, *6*, 643-655.
- [7] A. S. Brouwer, M. van den Broek, A. Seebregts, A. Faaij, *Renew. Sustain. Energy Rev* **2014**, *33*, 443-466.
- [8] IEA, **2020**: *World Energy Outlook 2020*, IEA, Paris, France. Retrieved from: <https://www.iea.org/reports/world-energy-outlook-2020>.

- [9] M. Yan, Y. Kawamata, P. S. Baran, *Chem. Rev.* **2017**, *117*, 13230-13319.
- [10] M. Yekini Suberu, M. Wazir Mustafa, N. Bashir, *Renew. Sustain. Energy Rev* **2014**, *35*, 499-514.
- [11] O. Gröger, H. A. Gasteiger, J.-P. Suchsland, *J. Electrochem. Soc.* **2015**, *162*, A2605-A2622.
- [12] A. Masias, J. Marcicki, W. A. Paxton, *ACS Energy Letters* **2021**, *6*, 621-630.
- [13] M. Marinaro, D. Bresser, E. Beyer, P. Faguy, K. Hosoi, H. Li, J. Sakovica, K. Amine, M. Wohlfahrt-Mehrens, S. Passerini, *J. Power Sources* **2020**, *459*, 228073.
- [14] W. R. Grove, *Philosophical Magazine Series 3* **1839**, *14*, 127-130.
- [15] Z. P. Cano, D. Banham, S. Ye, A. Hintennach, J. Lu, M. Fowler, Z. Chen, *Nat. Energy* **2018**, *3*, 279-289.
- [16] M. Bernt, A. Hartig-Weiß, M. F. Tovini, H. A. El-Sayed, C. Schramm, J. Schröter, C. Gebauer, H. A. Gasteiger, *Chem. Ing. Tech.* **2020**, *92*, 31-39.
- [17] E. Torres, M. Ayala, in *Comprehensive Inorganic Chemistry II (Second Edition)* (Eds.: Jan Reedijk, Kenneth Poeppelmeier), Elsevier, Amsterdam, **2013**, pp. 685-735.
- [18] A. J. Medford, A. Vojvodic, J. S. Hummelshøj, J. Voss, F. Abild-Pedersen, F. Studt, T. Bligaard, A. Nilsson, J. K. Nørskov, *J. Catal.* **2015**, *328*, 36-42.
- [19] J. K. Nørskov, J. Rossmeisl, A. Logadottir, L. Lindqvist, J. R. Kitchin, T. Bligaard, H. Jónsson, *J. Phys. Chem. B* **2004**, *108*, 17886-17892.
- [20] N. M. Marković, T. J. Schmidt, V. Stamenković, P. N. Ross, *Fuel Cells* **2001**, *1*, 105-116.
- [21] A. B. Laursen, A. S. Varela, F. Dionigi, H. Fanchiu, C. Miller, O. L. Trinhammer, J. Rossmeisl, S. Dahl, *J. Chem. Educ.* **2012**, *89*, 1595-1599.
- [22] V. Stamenkovic, B. S. Mun, K. J. J. Mayrhofer, P. N. Ross, N. M. Markovic, J. Rossmeisl, J. Greeley, J. K. Nørskov, *Angew. Chem. Int. Ed.* **2006**, *45*, 2897-2901.
- [23] Greeley, J. E. L. Stephens, A. S. Bondarenko, T. P. Johansson, H. A. Hansen, T. F. Jaramillo, Rossmeisl, J. Chorkendorff, J. K. Nørskov, *Nat Chem* **2009**, *1*, 552-556.
- [24] K. J. Waldron, J. C. Rutherford, D. Ford, N. J. Robinson, *Nature* **2009**, *460*, 823-830.
- [25] C. Andreini, I. Bertini, G. Cavallaro, G. L. Holliday, J. M. Thornton, *JBIC Journal of Biological Inorganic Chemistry* **2008**, *13*, 1205-1218.
- [26] G. Vaaje-Kolstad, B. Westereng, S. J. Horn, Z. Liu, H. Zhai, M. Sørlie, V. G. H. Eijsink, *Science* **2010**, *330*, 219-222.
- [27] G. Vaaje-Kolstad, Z. Forsberg, J. S. M. Loose, B. Bissaro, V. G. H. Eijsink, *Curr. Opin. Struct. Biol.* **2017**, *44*, 67-76.
- [28] K. E. H. Frandsen, et al., *Nat. Chem. Biol.* **2016**, *12*, 298-303.
- [29] G. R. Hemsworth, B. Henrissat, G. J. Davies, P. H. Walton, *Nat. Chem. Biol.* **2014**, *10*, 122-126.
- [30] B. Wang, P. H. Walton, C. Rovira, *ACS Catal.* **2019**, *9*, 4958-4969.
- [31] B. Wang, Z. Wang, G. J. Davies, P. H. Walton, C. Rovira, *ACS Catal.* **2020**, *10*, 12760-12769.
- [32] L. Ciano, G. J. Davies, W. B. Tolman, P. H. Walton, *Nat. Catal.* **2018**, *1*, 571-577.
- [33] M. O. Ross, F. MacMillan, J. Wang, A. Nisthal, T. J. Lawton, B. D. Olafson, S. L. Mayo, A. C. Rosenzweig, B. M. Hoffman, *Science* **2019**, *364*, 566-570.
- [34] E. I. Solomon, U. M. Sundaram, T. E. Machonkin, *Chem. Rev.* **1996**, *96*, 2563-2606.
- [35] E. I. Solomon, P. Chen, M. Metz, S.-K. Lee, A. E. Palmer, *Angew. Chem. Int. Ed.* **2001**, *40*, 4570-4590.
- [36] A. M. Mayer, R. C. Staples, *Phytochemistry* **2002**, *60*, 551-565.
- [37] J. P. Collman, N. K. Devaraj, R. A. Decréau, Y. Yang, Y.-L. Yan, W. Ebina, T. A. Eberspacher, C. E. D. Chidsey, *Science* **2007**, *315*, 1565-1568.
- [38] S. Chatterjee, K. Sengupta, S. Hematian, K. D. Karlin, A. Dey, *J. Am. Chem. Soc.* **2015**, *137*, 12897-12905.
- [39] S. M. Jones, E. I. Solomon, *Cell. Mol. Life Sci.* **2015**, *72*, 869-883.
- [40] L. Rulišek, U. Ryde, *Coord. Chem. Rev.* **2013**, *257*, 445-458.
- [41] S. C. Barton, H.-H. Kim, G. Binyamin, Y. Zhang, A. Heller, *J. Am. Chem. Soc.* **2001**, *123*, 5802-5803.
- [42] V. Soukharev, N. Mano, A. Heller, *J. Am. Chem. Soc.* **2004**, *126*, 8368-8369.
- [43] N. Mano, V. Soukharev, A. Heller, *J. Phys. Chem. B* **2006**, *110*, 11180-11187.
- [44] C. F. Blanford, R. S. Heath, F. A. Armstrong, *Chem. Commun.* **2007**, 1710-1712.
- [45] J. A. Cracknell, K. A. Vincent, F. A. Armstrong, *Chem. Rev.* **2008**, *108*, 2439-2461.
- [46] C. F. Blanford, C. E. Foster, R. S. Heath, F. A. Armstrong, *Faraday Discuss.* **2009**, *140*, 319-335.
- [47] M. S. Thorum, C. A. Anderson, J. J. Hatch, A. S. Campbell, N. M. Marshall, S. C. Zimmerman, Y. Lu, A. A.

- Gewirth, *J. Phys. Chem. Lett.* **2010**, *1*, 2251-2254.
- [48] S. Tsujimura, Y. Kamitaka, K. Kano, *Fuel Cells* **2007**, *7*, 463-469.
- [49] E. A. Lewis, W. B. Tolman, *Chem. Rev.* **2004**, *104*, 1047-1076.
- [50] J. A. Halfen, S. Mahapatra, E. C. Wilkinson, S. Kaderli, V. G. Young, L. Que, A. D. Zuberbühler, W. B. Tolman, *Science* **1996**, *271*, 1397-1400.
- [51] L. M. Mirica, X. Ottenwaelder, T. D. P. Stack, *Chem. Rev.* **2004**, *104*, 1013-1046.
- [52] I. Pecht, M. Anbar, *J. Chem. Soc. A* **1968**, 1902-1904.
- [53] A. L. Crumbliss, L. J. Gestaut, *J. Coord. Chem.* **1976**, *5*, 109-111.
- [54] C. E. Elwell, N. L. Gagnon, B. D. Neisen, D. Dhar, A. D. Spaeth, G. M. Yee, W. B. Tolman, *Chem. Rev.* **2017**, *117*, 2059-2107.
- [55] R. R. Jacobson, Z. Tyeklar, A. Farooq, K. D. Karlin, S. Liu, J. Zubieta, *J. Am. Chem. Soc.* **1988**, *110*, 3690-3692.
- [56] M. J. Baldwin, P. K. Ross, J. E. Pate, Z. Tyeklar, K. D. Karlin, E. I. Solomon, *J. Am. Chem. Soc.* **1991**, *113*, 8671-8679.
- [57] K. D. Karlin, N. Wei, B. Jung, S. Kaderli, P. Niklaus, A. D. Zuberbuehler, *J. Am. Chem. Soc.* **1993**, *115*, 9506-9514.
- [58] K. D. Karlin, S. Kaderli, A. D. Zuberbühler, *Acc. Chem. Res.* **1997**, *30*, 139-147.
- [59] C. X. Zhang, S. Kaderli, M. Costas, E.-i. Kim, Y.-M. Neuhold, K. D. Karlin, A. D. Zuberbühler, *Inorg. Chem.* **2003**, *42*, 1807-1824.
- [60] M. Schatz, et al., *Inorg. Chem.* **2001**, *40*, 2312-2322.
- [61] H. R. Lucas, L. Li, A. A. N. Sarjeant, M. A. Vance, E. I. Solomon, K. D. Karlin, *J. Am. Chem. Soc.* **2009**, *131*, 3230-3245.
- [62] H. R. Lucas, G. J. Meyer, K. D. Karlin, *J. Am. Chem. Soc.* **2010**, *132*, 12927-12940.
- [63] P. Comba, C. Haaf, S. Helmle, K. D. Karlin, S. Pandian, A. Waleska, *Inorg. Chem.* **2012**, *51*, 2841-2851.
- [64] M. T. Kieber-Emmons, J. W. Ginsbach, P. K. Wick, H. R. Lucas, M. E. Helton, B. Lucchese, M. Suzuki, A. D. Zuberbühler, K. D. Karlin, E. I. Solomon, *Angew. Chem. Int. Ed.* **2014**, *53*, 4935-4939.
- [65] I. Garcia-Bosch, R. E. Cowley, D. E. Díaz, M. A. Siegler, W. Nam, E. I. Solomon, K. D. Karlin, *Chem. Eur. J.* **2016**, *22*, 5133-5137.
- [66] I. López, R. Cao, D. A. Quist, K. D. Karlin, N. Le Poul, *Chem. Eur. J.* **2017**, *23*, 18314-18319.
- [67] V. E. Kazarinov, M. R. Tarasevich, K. A. Radyushkina, V. N. Andreev, *J. Electroanal. Chem.* **1979**, *100*, 225-232.
- [68] M. R. Tarasevich, K. A. Radyushkina, *Russ. Chem. Rev.* **1980**, *49*, 718-730.
- [69] P. Vasudevan, Santosh, N. Mann, S. Tyagi, *Transit Met Chem* **1990**, *15*, 81-90.
- [70] R. Jasinski, *Nature* **1964**, *201*, 1212-1213.
- [71] J. Zhang, F. C. Anson, *J. Electroanal. Chem.* **1992**, *341*, 323-341.
- [72] K. Shigehara, F. C. Anson, *J. Electroanal. Chem.* **1982**, *132*, 107-118.
- [73] J. Zhang, F. C. Anson, *J. Electroanal. Chem.* **1993**, *348*, 81-97.
- [74] J. Zhang, F. C. Anson, *Electrochim. Acta* **1993**, *38*, 2423-2429.
- [75] Y. Lei, F. C. Anson, *Inorg. Chem.* **1994**, *33*, 5003-5009.
- [76] C. C. L. McCrory, X. Ottenwaelder, T. D. P. Stack, C. E. D. Chidsey, *J. Phys. Chem. A* **2007**, *111*, 12641-12650.
- [77] C. C. L. McCrory, A. Devadoss, X. Ottenwaelder, R. D. Lowe, T. D. P. Stack, C. E. D. Chidsey, *J. Am. Chem. Soc.* **2011**, *133*, 3696-3699.
- [78] S. Fukuzumi, H. Kotani, H. R. Lucas, K. Doi, T. Suenobu, R. L. Peterson, K. D. Karlin, *J. Am. Chem. Soc.* **2010**, *132*, 6874-6875.
- [79] S. Fukuzumi, L. Tahsini, Y.-M. Lee, K. Ohkubo, W. Nam, K. D. Karlin, *J. Am. Chem. Soc.* **2012**, *134*, 7025-7035.
- [80] L. Tahsini, H. Kotani, Y. M. Lee, J. Cho, W. Nam, K. D. Karlin, S. Fukuzumi, *Chem. Eur. J.* **2012**, *18*, 1084-1093.
- [81] D. Das, Y.-M. Lee, K. Ohkubo, W. Nam, K. D. Karlin, S. Fukuzumi, *J. Am. Chem. Soc.* **2013**, *135*, 2825-2834.
- [82] D. Das, Y.-M. Lee, K. Ohkubo, W. Nam, K. D. Karlin, S. Fukuzumi, *J. Am. Chem. Soc.* **2013**, *135*, 4018-4026.
- [83] S. Kakuda, R. L. Peterson, K. Ohkubo, K. D. Karlin, S. Fukuzumi, *J. Am. Chem. Soc.* **2013**, *135*, 6513-6522.
- [84] M. A. Thorseth, C. S. Letko, T. B. Rauchfuss, A. A. Gewirth, *Inorg. Chem.* **2011**, *50*, 6158-6162.
- [85] M. A. Thorseth, C. S. Letko, E. C. M. Tse, T. B. Rauchfuss, A. A. Gewirth, *Inorg. Chem.* **2013**, *52*, 628-634.
- [86] E. C. M. Tse, D. Schilter, D. L. Gray, T. B. Rauchfuss, A. A. Gewirth, *Inorg. Chem.* **2014**, *53*, 8505-8516.
- [87] M. Asahi, S.-i. Yamazaki, S. Itoh, T. Ioroi, *Electrochim. Acta* **2016**, *211*, 193-198.

- [88] S. Fukuzumi, Y.-M. Lee, W. Nam, *ChemCatChem* **2018**, *10*, 9-28.
- [89] M. Asahi, S.-i. Yamazaki, S. Itoh, T. Ioroi, *Dalton Trans.* **2014**, *43*, 10705-10709.
- [90] M. Asahi, S.-i. Yamazaki, Y. Morimoto, S. Itoh, T. Ioroi, *Inorg. Chim. Acta* **2018**, *471*, 91-98.
- [91] Q. He, T. Mugadza, G. Hwang, T. Nyokong, *Int. J. Electrochem. Sci* **2012**, *7*, 7045-7064.
- [92] M. A. Thorseth, C. E. Tornow, E. C. M. Tse, A. A. Gewirth, *Coord. Chem. Rev.* **2013**, *257*, 130-139.
- [93] N. W. G. Smits, B. van Dijk, I. de Bruin, S. L. T. Groeneveld, M. A. Siegler, D. G. H. Hetterscheid, *Inorg. Chem.* **2020**, *59*, 16398-16409.
- [94] A. M. Appel, M. L. Helm, *ACS Catal.* **2014**, *4*, 630-633.
- [95] E. Aznar, S. Ferrer, J. Borrás, F. Lloret, M. Liu-González, H. Rodríguez-Prieto, S. García-Granda, *Eur. J. Inorg. Chem.* **2006**, *2006*, 5115-5125.
- [96] M. S. Thorum, J. Yadav, A. A. Gewirth, *Angew. Chem. Int. Ed.* **2009**, *48*, 165-167.
- [97] B. van Dijk, J. P. Hofmann, D. G. H. Hetterscheid, *Phys. Chem. Chem. Phys.* **2018**, *20*, 19625-19634.
- [98] V. Artero, J.-M. Saveant, *Energy Environ. Sci.* **2014**, *7*, 3808-3814.
- [99] C. Costentin, J.-M. Savéant, *ChemElectroChem* **2014**, *1*, 1226-1236.
- [100] C. Costentin, G. Passard, J.-M. Savéant, *J. Am. Chem. Soc.* **2015**, *137*, 5461-5467.
- [101] T. Bligaard, R. M. Bullock, C. T. Campbell, J. G. Chen, B. C. Gates, R. J. Gorte, C. W. Jones, W. D. Jones, J. R. Kitchin, S. L. Scott, *ACS Catal.* **2016**, *6*, 2590-2602.
- [102] R. Matheu, S. Neudeck, F. Meyer, X. Sala, A. Llobet, *ChemSusChem* **2016**, *9*, 3361-3369.
- [103] Y. Matsubara, *ACS Energy Letters* **2019**, *4*, 1999-2004.
- [104] K. J. Lee, N. Elgrishi, B. Kandemir, J. L. Dempsey, *Nat. Rev. Chem.* **2017**, *1*, 0039.
- [105] C. Costentin, J.-M. Savéant, *J. Am. Chem. Soc.* **2017**, *139*, 8245-8250.
- [106] J.-M. Saveant, *ChemElectroChem* **2016**, *3*, 1967-1977.
- [107] E. S. Rountree, B. D. McCarthy, T. T. Eisenhart, J. L. Dempsey, *Inorg. Chem.* **2014**, *53*, 9983-10002.
- [108] V. S. Thoi, Y. Sun, J. R. Long, C. J. Chang, *Chem. Soc. Rev.* **2013**, *42*, 2388-2400.
- [109] M. L. Pegis, C. F. Wise, D. J. Martin, J. M. Mayer, *Chem. Rev.* **2018**, *118*, 2340-2391.
- [110] J.-M. Savéant, *Chem. Rev.* **2008**, *108*, 2348-2378.
- [111] Q. Yin, J. M. Tan, C. Besson, Y. V. Geletii, D. G. Musaev, A. E. Kuznetsov, Z. Luo, K. I. Hardcastle, C. L. Hill, *Science* **2010**, *328*, 342-345.
- [112] S. M. Barnett, K. I. Goldberg, J. M. Mayer, *Nat Chem* **2012**, *4*, 498-502.
- [113] B. D. Matson, C. T. Carver, A. Von Ruden, J. Y. Yang, S. Raagei, J. M. Mayer, *Chem. Commun.* **2012**, *48*, 11100-11102.
- [114] C. Liu, H. Lei, Z. Zhang, F. Chen, R. Cao, *Chem. Commun.* **2017**, *53*, 3189-3192.
- [115] L.-L. Zhou, T. Fang, J.-P. Cao, Z.-H. Zhu, X.-T. Su, S.-Z. Zhan, *J. Power Sources* **2015**, *273*, 298-304.
- [116] J. J. Walsh, G. Neri, C. L. Smith, A. J. Cowan, *Organometallics* **2019**, *38*, 1224-1229.
- [117] Y. Han, Y. Wu, W. Lai, R. Cao, *Inorg. Chem.* **2015**, *54*, 5604-5613.
- [118] A. D. Wilson, R. H. Newell, M. J. McNevin, J. T. Muckerman, M. Rakowski DuBois, D. L. DuBois, *J. Am. Chem. Soc.* **2006**, *128*, 358-366.
- [119] G. A. N. Felton, R. S. Glass, D. L. Lichtenberger, D. H. Evans, *Inorg. Chem.* **2006**, *45*, 9181-9184.
- [120] V. Fourmond, P.-A. Jacques, M. Fontecave, V. Artero, *Inorg. Chem.* **2010**, *49*, 10338-10347.
- [121] J. A. S. Roberts, R. M. Bullock, *Inorg. Chem.* **2013**, *52*, 3823-3835.
- [122] M. L. Pegis, J. A. S. Roberts, D. J. Wasylenko, E. A. Mader, A. M. Appel, J. M. Mayer, *Inorg. Chem.* **2015**, *54*, 11883-11888.
- [123] C. Costentin, S. Drouet, M. Robert, J.-M. Savéant, *J. Am. Chem. Soc.* **2012**, *134*, 11235-11242.
- [124] V. C. C. Wang, B. A. Johnson, *ACS Catal.* **2019**, *9*, 7109-7123.
- [125] C. Costentin, D. G. Nocera, C. N. Brodsky, *Proc. Natl. Acad. Sci.* **2017**, *114*, 11303-11308.
- [126] C. Costentin, J.-M. Savéant, *Nat. Rev. Chem.* **2017**, *1*, 0087.
- [127] I. Azcarate, C. Costentin, M. Robert, J.-M. Savéant, *J. Phys. Chem. C* **2016**, *120*, 28951-28960.

